

Cu Nuclear Quadrupole Resonance Study of $\text{La}_{2-x}\text{Sr}_x\text{Cu}_{1-y}\text{Zn}_y\text{O}_4$ ($x=0.10, 0.15$ and 0.20): Zn-induced Wipeout Effect near the Magnetic and Electric Instability

H. Yamagata¹, H. Miyamoto¹, K. Nakamura¹, M. Matsumura¹, and Y. Itoh^{2,*}

¹*Department of Material Science, Faculty of Science, Kochi University, Kochi 780-8520, Japan*

²*Japan Society for the Promotion of Science, Tokyo, Japan*

(November 21, 2001)

We studied Zn-substitution effect on the high- T_c superconductors, underdoped $\text{La}_{2-x}\text{Sr}_x\text{Cu}_{1-y}\text{Zn}_y\text{O}_4$ ($x=0.10; y=0, 0.01, 0.02$), optimally doped ($x=0.15; y=0, 0.02$), and overdoped ($x=0.20; y=0, 0.03, 0.06$) in a temperature range of $T=4.2\text{-}300$ K, using Cu nuclear quadrupole resonance (NQR) spin-echo technique. We found full disappearance of the Cu NQR signals for the Zn-substituted, Sr-underdoped $x=0.10$ samples below about 40 K, partial disappearance for the Sr-optimally doped ones below about 50 K, but not for the overdoped $x=0.20$ ones. From the Zn-doping, the Sr-doping and the temperature dependence of the wipeout effect, we associate the wipeout effect with Zn-induced Curie magnetism or its extended glassy charge-spin stripe formation.

74.72.Dn, 76.60.-k, 75.20.Hr

I. INTRODUCTION

Nonmagnetic Zn^{2+} ion has a closed shell of the $3d$ electrons, so that it must not carry a local moment. However, the actual Zn substitution strongly suppresses the transition temperature T_c of underdoped high- T_c superconductors [1], induces a Curie-like uniform susceptibility [2–7], and finally causes a quasi-elastic magnetic correlation [8]. In contrast to a simple dilution effect, Yamagata, Inada and Matsumura discovered a significant loss of zero-field Cu nuclear quadrupole resonance (NQR) spectrum intensity (wipeout effect) for the Zn-impurity doped $\text{YBa}_2\text{Cu}_3\text{O}_{7-\delta}$ [9]. Subsequent muon spin relaxation study observed a Zn-induced magnetic fluctuation with a short relaxation time ($< 10 \mu\text{s}$) for the Zn-doped $\text{YBa}_2\text{Cu}_3\text{O}_y$ ($y=6.43\text{-}6.67$) [10], and inelastic neutron scattering study observed the Zn-induced low frequency spin fluctuations around an antiferromagnetic wave vector for the Zn-doped $\text{YBa}_2\text{Cu}_3\text{O}_{6.97}$ [11,12]. Much attention has been paid for the novel microscopic effect of Zn doping [13–15].

Here, the wipeout effect is defined as disappearance of the observable NMR or NQR signal around a rf frequency region in a longer time scale than a few μs . For the nuclear spin system in a material, the temperature dependence of the integrated NMR/NQR signal should follow a Curie law, because the nuclear spins in athermal equilibrium state follow the Boltzmann distribution. However, imperfection or impurity changes a spatial environment around the nuclei place by place, so that the NMR/NQR

spectrum is broadened or split into several pieces. The nuclei around a magnetic impurity feel a strong local field from the impurity, so that several neighbor nuclei surrounding the impurity are unobservable. The strong wipeout effects have been observed for the lightly doped insulators [16] and the Co-doped high- T_c superconductors [17]. From careful measurements of the Zn-doping dependence of the integrated Cu(2) NQR spectrum for $\text{YBa}_2\text{Cu}_3\text{O}_{7-\delta}$, the first neighbor shell surrounding the Zn-occupied Cu(2) site was inferred to be unobservable [9]. Similar observation is reported in refs. [18,13]. The strong wipeout effect has also been observed for the underdoped $\text{La}_{2-x}\text{Sr}_x\text{CuO}_4$ ($x \leq 0.125$), which is associated with a charge-stripe ordering or its glassy nature [19–21].

In this paper, we report Cu NQR spectrum measurements for Zn-doped $\text{La}_{2-x}\text{Sr}_x\text{Cu}_{1-y}\text{Zn}_y\text{O}_4$ with (Sr-underdoped $x=0.10; y=0, 0.01, 0.02$), (optimally Sr-doped $x=0.15; y=0, 0.02$), and (Sr-overdoped $x=0.20; y=0, 0.03, 0.06$) in a temperature range of $T=4.2\text{-}300$ K. We found that an enhanced wipeout effect due to the Zn doping occurs in the Sr-underdoped samples but not for the overdoped ones. For the Zn-doped $x=0.10$ sample, the Cu NQR signal completely diminishes below about 40 K. The diminished NQR signal recovers from the Sr-underdoped to the overdoped regimes. From the Sr-doping dependence of the Zn-induced wipeout effect and the temperature dependence of the wipeout effect from the normal to the superconducting states, we discuss the origin of the Zn-enhanced wipeout effect.

II. EXPERIMENTS

Polycrystalline samples were synthesized by a conventional solid-state-reaction method from CuO , ZnO , SrCO_3 , and La_2O_3 , as described in refs. [22,23]. The X-ray diffraction patterns indicated single phases. Nearly the same amount of samples (about 1.8 g of fine powders with grain radii less than about 20 nm), so as to include nearly the same number of the Cu sites, were prepared for the NQR measurements. All the samples for Cu NQR measurement were coated by paraffin oil. T_c was determined from polycrystalline resistivity. In Fig. 1, T_c is plotted as a function of Zn content y for Sr doping of $x=0.10, 0.15$ and 0.20 . The error bars are estimated from the onset of resistivity drop and zero re-

sistivity. $\Delta T_c/\Delta(100y)$ is estimated to be -16 K/% for $x=0.10$, -13 K/% for $x=0.15$, and -7 K/% for $x=0.20$, which are similar to the reported values [11]. Zn doping suppresses T_c of the underdoped materials stronger than of the overdoped ones. The critical impurity concentration y_c ($T_c < 4.2$ K) is estimated to be about 0.019 for $x=0.10$ and about 0.042 for $x=0.20$.

A home-made, phase-coherent-type pulsed spectrometer was utilized to do Cu NQR experiments. The Cu NQR frequency spectra with quadrature detection were measured by integration of Cu nuclear spin-echoes with changing the frequency point by point in a two-pulse sequence ($\pi/2$ - τ - π -echo). Transverse relaxation curves of the Cu nuclear spin-echo $E(\tau)$ were also measured by the two-pulse method. A typical width of the first exciting $\pi/2$ -pulse t_W was about 1 μ s (the pulse strength $\nu_1 \sim 250$ kHz from $2\pi\nu_1 t_W = \pi/2$, or $H_1 \sim 128$ G from $3\gamma_n H_1 t_W = \pi/2$ with the ^{63}Cu nuclear gyromagnetic ratio γ_n), the time interval τ for the NQR spectrum measurement was about 8~12 μ s, and the number of averaging times of spin-echos was about 1000.

III. EXPERIMENTAL RESULTS

Figure 2 shows the temperature dependence of the Cu NQR spectra of the Sr-underdoped $\text{La}_{1.9}\text{Sr}_{0.1}\text{Cu}_{1-y}\text{Zn}_y\text{O}_4$ with Zn doping of $y=0, 0.01, 0.02$ (left) and of the Sr-overdoped $\text{La}_{1.8}\text{Sr}_{0.2}\text{Cu}_{1-y}\text{Zn}_y\text{O}_4$ with Zn doping of $y=0, 0.03, 0.06$ (right), at $T=77$ K (top), 30 or 35 K (middle), and 4.2 K (bottom). The observed Cu NQR spectra for Zn-free materials agree with the reported ones [24,25], which are understood by two sets (A and B) of $^{63,65}\text{Cu}$ NQR lines (the natural abundance ratio of $^{63}\text{Cu}/^{65}\text{Cu}=0.69/0.31$, and the resonance frequency ratio of $^{63}\nu_Q/^{65}\nu_Q = 0.211/0.195$). The site assignment to A and B lines is given in refs. [24,25]. Obviously, Zn causes a strong wipeout effect for the underdoped materials at lower temperatures. Although some decrease of the Cu NQR spectrum has been reported for the Zn-free $x=0.10$ [19], we found that the Cu NQR signals completely vanish at 4.2 K both for the Zn-doped but finite T_c sample ($T_c=13$ K, $y=0.01$) and for the Zn-doped, non-superconducting one ($T_c < 4.2$ K, $y=0.02$). However, Zn does not seem to affect the Cu NQR spectrum of the overdoped ones. Thus, Zn effect is quite different between the underdoped and the overdoped regimes.

Figure 3 shows the temperature dependence of transverse relaxation rates, Lorentzian decay rates $1/T_{2L}$ (closed circles) and Gaussian decay rates $1/T_{2G}$ (open triangles), of the ^{63}Cu (A) nuclear spin-echo decays (a) for the Zn-free $x=0.10$ and (b) for the Zn-doped $x=0.10$ ($y=0.02$), and (c) for the Zn-free $x=0.20$ and (d) for the Zn-doped $x=0.20$ ($y=0.06$). The relaxation times T_{2L} and T_{2G} were obtained from the least-squares fitting of

a Gaussian-times-Lorentzian function $E(\tau) = E(0)\exp[-0.5(2\tau/T_{2G})^2 - (2\tau/T_{2L})]$ ($E(0)$, T_{2L} and T_{2G} are the fitting parameters) to the experimental decay curves $E(\tau)$. The Lorentzian component is predominant at low temperatures, which agrees with the previous similar report in the wipeout effect [19]. The magnitudes of $1/T_{2L}$ and $1/T_{2G}$ increase with decreasing Sr content. A decrease of $1/T_{2L}$ at T_c in (a) and (c) starts at the onset of superconductivity both for the Zn-free $x=0.10$ and 0.20 ($T_c \sim 29$ K). As the temperature decreases, the significant loss of the Cu NQR spectra occurs as in Fig. 2; nevertheless any strong divergence of the transverse relaxation rates was not observed for the Zn-doped, Sr-underdoped sample in (b). For the Zn-doped, Sr-overdoped one in (d), an increase of $1/T_{2L}$ was observed down to 4.2 K below the Zn-free $T_c \sim 29$ K.

Figure 4 shows a typical separation of an observed Cu NQR spectrum of the $(x, y)=(0.15, 0.02)$ sample at 4.2 K into two sets (A and B) of $^{63,65}\text{Cu}$ NQR lines by Gaussian distribution functions (solid curves). The fitting procedure is the same as those in refs. [24,25].

In Fig. 5, the estimated full-width at half maximum (FWHM) of ^{63}Cu (A) NQR line is shown for $x=0.10$ ($y=0, 0.01, 0.02$) (left) and for $x=0.20$ ($y=0, 0.03, 0.06$) (right). The estimated FWHM is about ~ 2.0 MHz for $x=0.10$ and ~ 2.2 MHz for $x=0.20$ above $T=100$, which seem to be independent of the Zn content y . At lower temperatures than about 100 K, the linewidth is slightly broadened to be ~ 2.3 MHz for both x .

Figure 6 shows the temperature dependence of the integrated intensity multiplied by temperature $I(x=0.10, y)$, $I(x=0.15, y)$ and $I(x=0.2, y)$ for the Zn-free and Zn-doped samples. Figure 7 shows the ratio of the integrated Cu NQR spectra, $I(x=0.10, y=0.01, 0.02)/I(x=0.10, y=0)$, $I(x=0.15, y=0.02)/I(x=0.15, y=0)$, and $I(x=0.20, y=0.03, 0.06)/I(x=0.20, y=0)$ (from the top to the bottom) as functions of temperature. Each integrated Cu NQR spectrum $I(x, y)$ was corrected by a Boltzmann factor ($1/T$) and was extrapolated to $\tau \rightarrow 0$ by using the Gaussian-times-Lorentzian function with the decay times in Fig. 3 [for the $(x, y)=(0.15, 0.02)$ sample, the decay curve at 4.2 K was reproduced by a two-exponential function better than the Gaussian-times-Lorentzian, so that only $I(x=0.15, y=0.02)$ at 4.2 K was extrapolated by a two-exponential function].

As shown in Fig. 6, for the Zn-free $x=0.10$ sample, the Cu NQR spectrum decreases monotonically below 50 K to 4.2 K, being consistent with the result in ref. [19]. This behavior is not observed for the Zn-free optimally doped $x=0.15$ and overdoped $x=0.20$ samples, whose Cu NQR signals increase with following a Boltzmann factor. In a higher temperature range of $T=100$ -300 K, about 20 to 30 % of the Cu NQR signal is wiped out with substituting Zn impurities for $x=0.10$ and $x=0.15$ samples, while for overdoped ones ($x=0.20$) the strong wipeout is not observed in a whole temperature range. By using the

intensity ratio, one can observe a relative intensity loss of the Cu NQR spectrum at each temperature as shown in Fig. 7. For the Zn-doped underdoped $x=0.10$ samples, the Cu NQR spectrum completely disappears below about 40 K. For the Zn-doped optimal $x=0.15$ samples, the wipeout effect is incomplete even at 4.2 K. For the Zn-doped overdoped $x=0.20$ samples, any loss of the signal intensity more than the site substitution is not observed.

IV. DISCUSSIONS

A. Sr-underdoping-induced wipeout effect and Zn-induced wipeout effect

The strong wipeout effect has already been observed for the Zn-free, deeply Sr-underdoped $\text{La}_{2-x}\text{Sr}_x\text{CuO}_4$ ($1/16 < x < 1/8$), which is associated with the charge-spin stripe ordering [19] or the glassy slowing-down charge-spin fluctuations with distributed spin fluctuation energy constants [20]. The charge-spin stripe ordering is theoretically proposed for doped Mott insulators [26], which is experimentally confirmed to be stabilized for a specific composition [27,28].

The Zn-induced wipeout effect, additionally for $x=0.10$ but newly for $x=0.15$, is not due to a simple lattice disorder, because any large broadening of the line width or change of the line shape is not observed. For $x=0.15$, the temperature dependent wipeout effect is obviously observed with Zn doping, which does not exist in the pure ($x=0.15, y=0$). Thus, the wipeout effect for optimally doped samples of $x=0.15$ is a purely Zn-induced wipeout effect.

When the charge-spin stripe ordering is *static* at low temperatures, one must observe some pattern in a Zeeman-perturbed Cu NQR spectrum, broadened by an internal magnetic field up to about 85 MHz, as has actually been observed for a specific composition, i.e. $\text{La}_{2-x}\text{Ba}_x\text{CuO}_4$ with $x \sim 1/8$ [29,20], $\text{La}_{2-x-y}\text{Sr}_x\text{Y}_y\text{CuO}_4$ with $x=1/8$ [30], and $\text{La}_{2-x-y}\text{Eu}_y\text{Sr}_x\text{CuO}_4$ [31,32,20]. For the Zn-doped samples, however, we did not observe any escaped signal at lower or higher frequency regions than those in Fig. 2 down to 1.3 K. We also did not observe any large change of the line shape nor the line width as in Figs. 2 and 5. Thus, even if the stripe fluctuations exhibit slowing down behavior at 40 K, it must keep the *quasi-static* nature down to 1.3 K. The temperature dependence of Cu NQR intensity could not tell us whether the wipeout sites make a stripe pattern or a random distribution on the CuO_2 plane in real space. Direct spatial information is lack in the Cu NQR intensity.

From previous works [19,20], it is shown that there is strong wipeout effect in an extensive Sr concentration region ($1/16 < x < 1/8$) without Zn impurities. Then, the Zn substitution effect may help to extend the wipeout

region up to $x=0.15$ and to increase the wipeout fraction more than the samples of $y=0$. This is similar to Nd- or Eu-codoping effect. For Nd- or Eu-codoped samples, the optimal T_c with respect to x is suppressed, the specific T_c suppression region around $x=1/8$ is broadened, and then the wipeout region is extended into the overdoping region up to $x=0.20$ [20]. For Zn-substituted samples, the superconductivity itself is also suppressed, and the wipeout region is also extended up to $x=0.15$. However, one should notice that there is a difference between the Sr-underdoping effect and the Zn-induced effect. The Zn impurities induce Curie magnetism but not the Sr underdoping [2–5]. The Zn doping readily induces a Curie-like uniform susceptibility for underdoped $\text{YBa}_2\text{Cu}_{3-x}\text{Zn}_x\text{O}_{7-\delta}$, which is assigned to local moments induced by Zn through ^{89}Y NMR study [14]. The Zn impurity induces satellites of ^{89}Y NMR spectrum, which is not thought of the stripe pattern as in the $x=1/8$ systems [29–32,20]. The Curie-like uniform susceptibility is also observed for $\text{La}_{2-x}\text{Sr}_x\text{Cu}_{1-y}\text{Zn}_y\text{O}_4$ [2–5]. The observed strong wipeout effect due to Zn doping closely resembles that due to dilute magnetic alloys [33]. Thus, it is likely that Zn induces local moments near Zn and causes the strong wipeout effect in $\text{La}_{2-x}\text{Sr}_x\text{CuO}_4$. The Zn-induced Curie magnetism may extend a glassy state, similarly to the glassy stripe fluctuations. These results are sharply contrast to what is expected from a simple dilution effect, a dilute potential scattering for a Fermi liquid or normal residual density of states in a pair-breaking theory [34].

B. Wipeout effect without precursor

The abrupt wipeout effect without any precursor is one of the characteristics of the Zn-doping effect. The Cu NQR signal vanishes fully or partially without divergence of the linewidth nor of $1/T_2$ around the onset temperature T_{NQR} ($=40\sim 60$ K) of the wipeout effect. Unobservable nuclei suddenly increase at T_{NQR} . This anomaly is not a conventional second order magnetic long-range ordering. One may speculate that the low temperature electronic state on the CuO_2 plane is microscopically and spatially segregated, so as to make it impossible to transfer information of electronic states from the unobserved sites to the observed ones. Such a segregated electronic state being close to an antiferromagnetic instability is theoretically possible, if the superconductivity-to-antiferromagnetism transition is of first order [35]. The Mott transition is believed to be of first order.

Let us illustrate schematically a model on spin fluctuations in Fig. 8, through the time spectrum of a muon spin relaxation $M(t)$ (a) and the dynamical spin susceptibility $\chi''(Q_{in}, \omega)$ as a function of frequency ω (Q_{in} is an incommensurate wave vector) (b), which are inferred from the wipeout effect without any precursor below T_{NQR} .

The arrows indicate the respective changes when cooling down below T_{NQR} . In Fig. 8(a), the dashed curves are extrapolated from longer relaxation components. Figure 8(a) shows the appearance of a fast relaxation component ($< 5 \mu\text{s}$) at lower temperatures. In Fig. 8(b), the shaded area is an observable NQR frequency region. The spin fluctuations peaked at a low frequency ($\sim 30 \text{ MHz}$) and at a high frequency ($\geq 10^6 \text{ MHz}$) in Fig. 8(b) correspond to fast and slow relaxation components in Fig. 8(a), respectively. The present Cu NQR technique cannot detect such a fast relaxation component ($< 5 \mu\text{s}$) in Fig. 8(a).

This model is qualitatively evidenced by recent muon spin relaxation (μSR) [36] and inelastic neutron experiments [37]. The systematic study by muon spin relaxation for $\text{La}_{2-x}\text{Sr}_x\text{Cu}_{1-y}\text{Zn}_y\text{O}_4$ with extensive (x, y) -compositions indicates the existence of two characteristic temperatures T_f and T_g ($T_f > T_g$) [36]. With cooling down, a slowing down component in the spin fluctuations grows, first enters the μSR time window at T_f and then freezes into a glassy state at T_g . These characteristic temperatures depend on the hole and Zn concentrations and go to zero at $x=0.2$ irrespective of Zn concentration. Up to $x=0.2$ both T_f and T_g increase with increasing Zn concentration. After refs. [19,20], considering the difference in the time scales between NQR and μSR , our results are consistent with μSR ; the observed full wipeout effect on Cu NQR for $x=0.10$ agrees with appearance of the short relaxation component with a dominant fraction below $T_{NQR} \sim T_f$. Recent inelastic neutron scattering study for the optimally Sr-doped $\text{La}_{1.85}\text{Sr}_{0.15}\text{Cu}_{1-y}\text{Zn}_y\text{O}_4$, indicates that a small amount of Zn impurities strongly modifies the dynamical spin susceptibility $\chi''(\omega)$; a new in-gap state is induced by Zn at low temperatures [37]. This can result in a fast relaxation component in Cu nuclear relaxation. Unfortunately, the weight shift between the in-gap state and the original or the higher frequency spin susceptibility is not estimated within the existing data. In ref. [20], the large distribution function with respect to spin fluctuation energy is introduced to account consistently for a short nuclear spin-lattice relaxation time T_1 of ^{139}La NQR and a moderate T_1 of Cu NQR. Our model with a short and a long relaxation times is in parallel to such a distribution model.

V. CONCLUSION

We observed Zn-induced wipeout effect in addition to already-known strong wipeout effect for underdoped $\text{La}_{1.9}\text{Sr}_{0.1}\text{CuO}_4$, purely Zn-induced wipeout effect for optimally doped $\text{La}_{1.85}\text{Sr}_{0.15}\text{CuO}_4$, but small effect for overdoped $\text{La}_{1.8}\text{Sr}_{0.2}\text{CuO}_4$. The abrupt wipeout effect without any precursor, one of the characteristics of the Zn-doping effect, suggests appearance of a spatially segregated electronic state at low temperatures. We associate this strong wipeout effect with the Zn-induced Curie

magnetism or its extended effect of the glassy charge-spin stripe formation. Simultaneous magnetic and electric instability plays a key role in understanding the novel response quite sensitive to nonmagnetic Zn impurity.

VI. ACKNOWLEDGMENTS

We would like to thanks Y. Koike, C. Panagopoulos, H. Kimura, and K. Hirota for helpful discussions, and R. E. Walstedt for critical reading of the manuscript and kind detailed comments.

-
- * Present address: Superconductivity Research Laboratory, International Superconductivity Technology Center, 1-10-13 Shinonome, Koto-ku Tokyo 135-0062, Japan
- [1] G. Xiao, M. Z. Cieplak, D. Musser, A. Gavrin, F. H. Streitz, C. L. Chien, J. J. Rhyne, J. A. Gotaas: *Nature* **332** (1988) 238.
 - [2] G. Xiao, M. Z. Cieplak, J. Q. Xiao and C. L. Chien: *Phys. Rev.* **B42** (1990) 8752.
 - [3] G. Xiao, M. Z. Cieplak and C. L. Chien: *Phys. Rev. B* **42** (1990) 240.
 - [4] H. Harashina, T. Nishikawa, T. Kiyokura, S. Shamoto, M. Sato, and K. Kakurai: *Physica C* **212** (1993) 142.
 - [5] P. Monod, S. Zagoulaev, and J. Jegoudez: *Physica C* **259** (1996) 271.
 - [6] H. Alloul, P. Mendels, H. Casalta, J. F. Marucco, and J. Arabski: *Phys. Rev. Lett.* **67** (1991) 3140.
 - [7] P. Mendels, J. Bobroff, G. Collin, H. Alloul, M. Gabay, J. F. Marucco, N. Blanchard, and B. Grenier: *Europhys. Lett.* **46** (1999) 678.
 - [8] K. Hirota, K. Yamada, I. Tanaka, and H. Kojima: *Physica B* **241-243** (1998) 817.
 - [9] H. Yamagata, K. Inada, and M. Matsumura: *Physica C* **185-189** (1991) 1101.
 - [10] P. Mendels, H. Alloul, J. H. Brewer, G. D. Morris, T. L. Duty, S. Johnston, E. J. Ansaldo, G. Collin, J. F. Marucco, C. Niedermayer, D. R. Noakes, and C. E. Stronach: *Phys. Rev. B* **49** (1994) 10035.
 - [11] H. Harashina, S. Shamoto, T. Kiyokura, M. Sato, K. Kakurai, and G. Shirane: *J. Phys. Soc. Jpn.* **62** (1993) 4009.
 - [12] Y. Sidis, P. Bourges, B. Hennion, L. P. Regnault, R. Villeneuve, G. Collin, and J.-F. Marucco: *Phys. Rev. B* **53** (1996) 6811.
 - [13] R. E. Walstedt, R. F. Bell, L. F. Schneemeyer, J. V. Waszczak, W. W. Warren, Jr., R. Dupree and A. Gencten: *Phys. Rev. B* **48** (1993) 10646.
 - [14] A. V. Mahajan, H. Alloul, G. Collin and J.-F. Marucco: *Phys. Rev. Lett.* **72** (1994) 3100.
 - [15] Y. Itoh, T. Machi, N. Watanabe, and N. Koshizuka: *J. Phys. Soc. Jpn.* **70** (2001) 644.
 - [16] M. Matsumura, H. Yamagata, Y. Yamada, K. Ishida, Y.

- Kitaoka, K. Asayama, H. Takagi, H. Iwabuchi, and S. Uchida: *J. Phys. Soc. Jpn.* **57** (1988) 3297.
- [17] M. Matsumura, Y. Takayanagi, H. Yamagata, and Y. Oda: *J. Phys. Soc. Jpn.* **63** (1994) 2382.
- [18] R. E. Walstedt, and W. W. Warren, jr.: *Appl. Magn. Reson.* **3** (1992) 469.
- [19] A. W. Hunt, P. M. Singer, K. R. Thurber, and T. Imai: *Phys. Rev. Lett.* **82** (1999) 4300.
- [20] A. W. Hunt, P. M. Singer, A. F. Cederstrom, and T. Imai: *Phys. Rev. B* **64** (2001) 134525.
- [21] M. H. Julien, A. Campana, A. Rigamonti, P. Carretta, F. Borsa, P. Kuhns, A. P. Reyes, W. G. Moulton, M. Horvatic, C. Berthier, A. Vietkin, and A. Revcolevschi: *Phys. Rev. B* **63** (2001) 144508.
- [22] K. Yoshimura, Y. Nishizawa, Y. Ueda, and K. Kosuge: *J. Phys. Soc. Jpn.* **59** (1990) 3073.
- [23] Y. Itoh, M. Matsumura, and H. Yamagata: *J. Phys. Soc. Jpn.* **65** (1996) 3747.
- [24] K. Yoshimura, T. Imai, T. Shimizu, Y. Ueda, K. Kosuge, and H. Yasuoka: *J. Phys. Soc. Jpn.* **58** (1989) 3057.
- [25] K. Yoshimura, T. Uemura, M. Kato, K. Kosuge, T. Imai, and H. Yasuoka: *Hyperfine Interactions* **79** (1993) 867.
- [26] J. Zaanen: *J. Phys. Chem. Solids* **59** (1998) 1760.
- [27] J. M. Tranquada, B. J. Sternlieb, J. D. Axe, Y. Nakamura, and S. Uchida: *Nature (London)* **375** (1995) 561.
- [28] J. M. Tranquada, N. Ichikawa, and S. Uchida: *Phys. Rev. B* **59** (1999) 14712.
- [29] M. Matsumura, T. Ikeda, and H. Yamagata: *J. Phys. Soc. Jpn.* **69** (2000) 1023.
- [30] M. Matsumura, K. Inouchi, H. Yamagata, and M. Sera: *Physica C* **357-360** (2001) 89.
- [31] T. Sawa, M. Matsumura, and H. Yamagata: *J. Phys. Soc. Jpn.* **70** (2001) 3503.
- [32] G. B. Teitelbaum, B. Buchner, and H. de Gronckel: *Phys. Rev. Lett.* **84** (2000) 2949.
- [33] H. Nagasawa, and W. A. Steyert: *J. Phys. Soc. Jpn.* **28** (1970) 1202.
- [34] T. Hotta: *J. Phys. Soc. Jpn.* **62** (1993) 274.
- [35] H. Kohno, H. Fukuyama, and M. Sigrist: *J. Phys. Soc. Jpn.* **68** (1999) 1500.
- [36] C. Panagopoulos, J. L. Tallon, B. D. Rainford, T. Xiang, J. R. Cooper, and C. A. Scott: *Phys. Rev. Lett. B* **66** (2002) 64501.
- [37] H. Kimura, M. Kofu, Y. Matsumoto, and K. Hirota: cond-mat/0209428 (unpublished work).

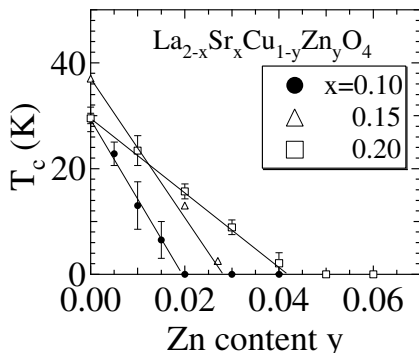


FIG. 1. Zn-doping dependence of T_c of $\text{La}_{2-x}\text{Sr}_x\text{Cu}_{1-y}\text{Zn}_y\text{O}_4$ with Sr contents of $x=0.10$, 0.15 , and 0.20 . The amount of the Zn impurity to diminish T_c is estimated to be $y_c=0.019$, 0.028 , and 0.042 for $x=0.10$, 0.15 , and 0.20 , respectively.

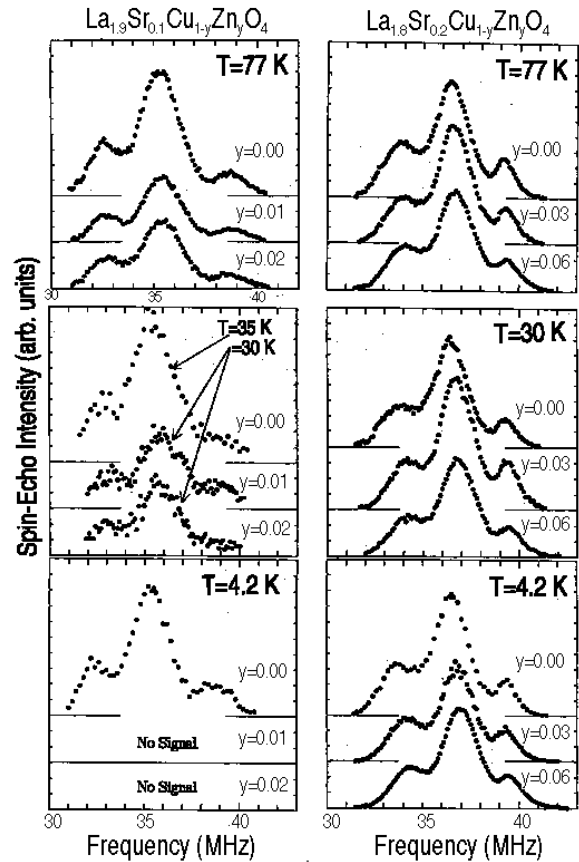


FIG. 2. Temperature dependence of Cu NQR frequency spectra of the Zn-doped, Sr-undersaturated samples with $x=0.10$ (Zn contents of $y=0$, 0.01 , and 0.02) (left) and of the Zn-doped, Sr-oversaturated samples with $x=0.20$ (Zn contents of $y=0$, 0.03 , and 0.06) (right), at $T=77$ K, 30 or 35 K and 4.2 K (from the top to the bottom). The Cu NQR signals for the Zn-doped, Sr-undersaturated samples completely diminished at lower temperatures.

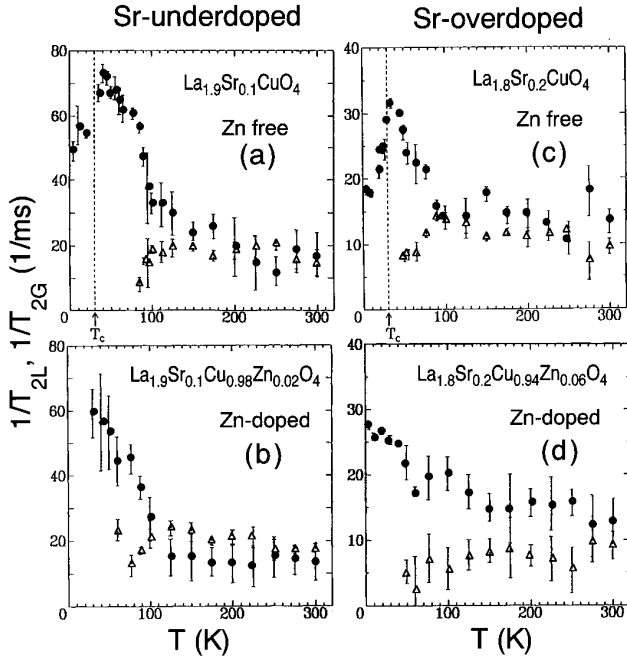


FIG. 3. Transverse relaxation rates, Lorentzian decay rates $1/T_{2L}$ (closed circles) and Gaussian decay rates $1/T_{2G}$ (open triangles), of the Cu nuclear spin-echo decays at each peak frequency for the Sr-underdoped (left) and the Sr-overdoped samples (right). For the Zn-free superconducting samples in (a) and (c), the decrease of the Lorentzian decay rate $1/T_{2L}$ is observed below T_c , irrespective of the wipeout effect. For the Zn-doped, Sr-underdoped sample in (b), no sizable divergence of $1/T_{2L}$ nor $1/T_{2G}$ is observed, when the Cu NQR signal diminishes at lower temperature. For the Zn-doped, Sr-overdoped sample in (d), $1/T_{2L}$ continues to increase below Zn-free T_c .

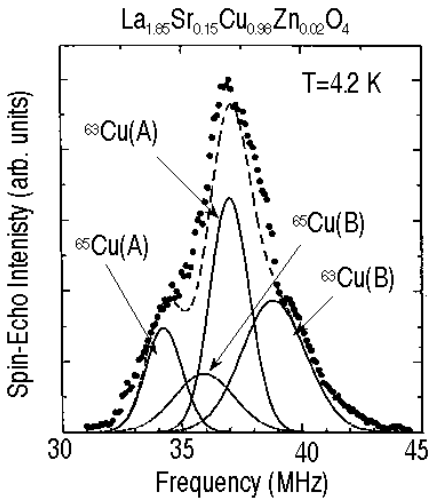


FIG. 4. A typical Cu NQR spectrum and the fitted results by the multiple Gaussian functions for $\text{La}_{1.85}\text{Sr}_{0.15}\text{Cu}_{0.98}\text{Zn}_{0.02}\text{O}_4$ at 4.2 K.

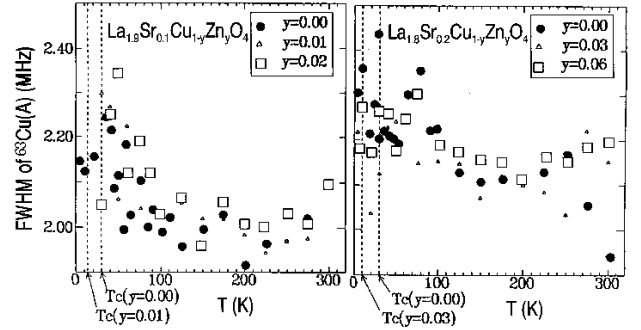


FIG. 5. The temperature dependence of the full-width of half maximum of $^{63}\text{Cu(A)}$. Some broadening is seen at low temperatures.

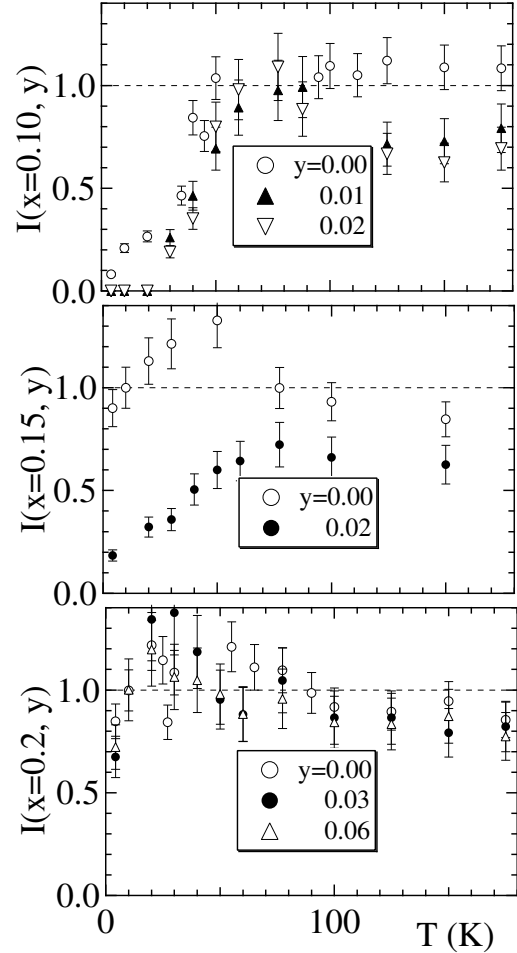


FIG. 6. The temperature dependence of the integrated intensity multiplied by temperature $I(x=0.10, y)$, $I(x=0.15, y)$, and $I(x=0.2, y)$ for the Zn-free and Zn-doped samples.

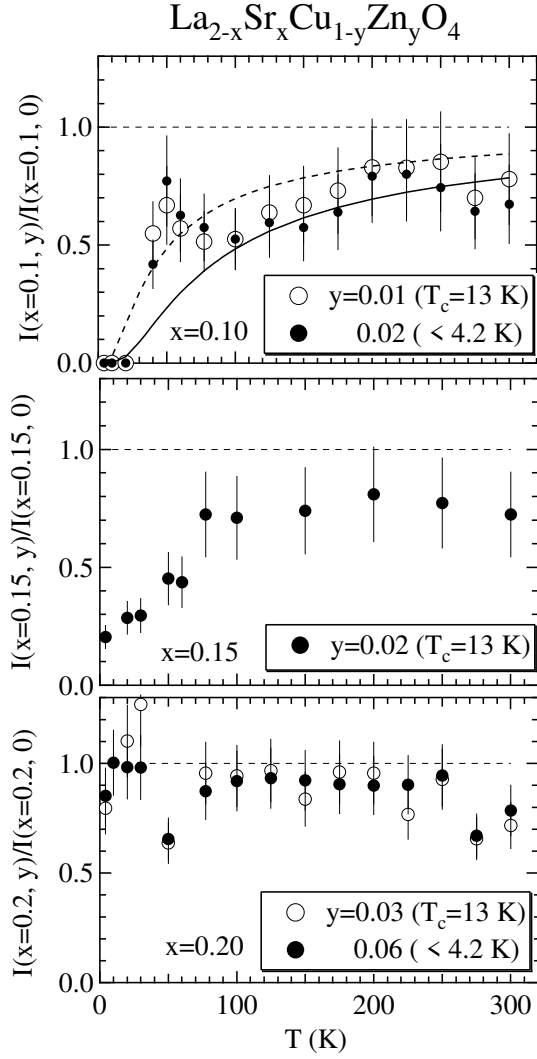


FIG. 7. The ratio of the integrated Cu NQR spectra, $I(x, y)/I(x, 0)$ with $(x=0.10; y=0, 0.01, 0.02)$ (top), $(x=0.15; y=0, 0.02)$ (middle) and $(x=0.20; y=0, 0.03, 0.06)$ (bottom), as functions of temperature. The dashed curve is a function of $(1-0.01)^{12 \times 300/T}$ and the solid one is $(1-0.02)^{12 \times 300/T}$. The function of $(1-x)^{\Sigma n.n.}$ is a probability of finding the nuclei under an assumption that the Curie-type temperature dependent region around Zn is wiped out (the third nearest-neighbor sites to Zn are assumed to be unobservable at $T=300$ K).

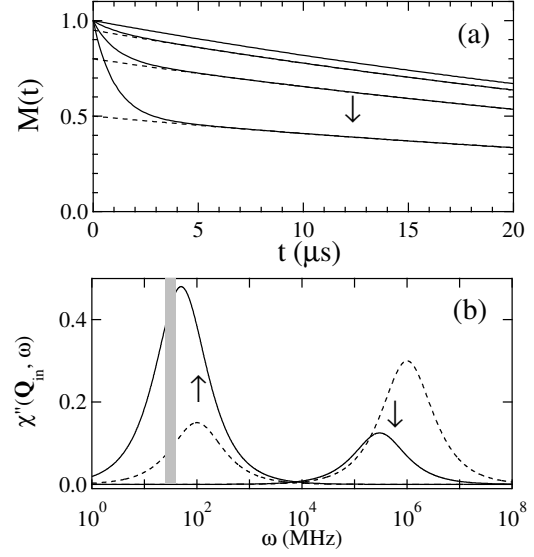


FIG. 8. A toy model to describe the full wipeout effect without any precursor below T_{NQR} . Schematic illustrations of the time spectrum of a muon spin relaxation $M(t)$ (a) and of the dynamical spin susceptibility $\chi''(\mathbf{Q}_{in}, \omega)$ (\mathbf{Q}_{in} is an incommensurate wave vector) (b). The arrows indicate cooling down below T_{NQR} . In Fig. 7(a), the dashed curves are extrapolated from longer relaxation components. In Fig. 7(b), the shaded area is an observable NQR frequency region.